Light Scattering Study of Polydimethyl Siloxane in Liquid and Supercritical Carbon Dioxide†

Pascal André,‡ Sarah L. Folk,‡ Mireille Adam,*,‡ Michael Rubinstein,*,‡ and Joseph M. DeSimone*,‡,§

Department of Chemistry, University of North Carolina at Chapel Hill, Chapel Hill, North Carolina 27599-3290, and Department of Chemical Engineering, North Carolina State University, Raleigh, North Carolina 27695-7905

Received: April 29, 2004; In Final Form: August 9, 2004

In this paper, we report the results of static and dynamic light scattering investigations of polydimethyl siloxane (PDMS) solutions in both liquid and supercritical carbon dioxide (CO_2). This study was performed below the theta point and provides quantitative information on the CO_2 solvent quality over a large range of temperature (25−54 °C) and density (0.97−1.01 g/mL). The solvent quality of the CO_2 can be adjusted by independently varying temperature or density, as demonstrated by the dependence of the second virial coefficient on these two parameters. The theta temperature was observed to be a strong function of CO_2 density and may be a weak function of the PDMS molecular weight. The strength of the excluded volume interactions in the PDMS−CO_2 solution was determined to be weaker than predicted, and no universal behavior was observed.

I. Introduction

Carbon dioxide (CO_2) is a byproduct of many industrial processes. It has many desirable characteristics, including being naturally occurring, nontoxic, nonflammable, and thus it seems to be an environmentally friendly alternative to reduce large quantities of solvent and water waste generated by industrial processes. Liquid and supercritical CO_2 can have gaslike viscosities and liquidlike densities. The advantages of the utilization of supercritical CO_2, as compared to other supercritical fluids, include its accessible critical temperature and pressure ($T_{critical} = 31$ °C; $P_{critical} = 72.8$ atm),[1] its environmental friendliness, its nonflammability, and its inertness to many chemical reactions.

Various applications for liquid and supercritical CO_2 have recently been highlighted in the literature, including the polymerization of various monomers, especially fluoroolefins, low-surface-energy coatings, and the design of resist materials with low absorbance at 193 and 157 nm in the field of microlithography.[2−4] For the successful use of compressed CO_2 processes, however, knowledge about the solution properties of the binary systems is still necessary. For industrial applications, a thorough understanding of solvent quality is key. Most polymeric species are insoluble in CO_2.[5] Amorphous fluoropolymers[5,6] and polysiloxanes[5] have been observed to be soluble in dense CO_2 over a large range of easily accessible experimental conditions. In addition, some reports have claimed limited solubility of some oligomeric materials, including poly(ether carbonates)[7] and poly(propylene oxide).[8]

Scattering techniques allow for the measurement of solvent quality through the determination of the second virial coefficient A_2, which is a thermodynamic parameter that is related to the relative strength of polymer−polymer versus polymer−solvent interactions. A_2 has been measured by either static light scattering (SLS)[11−14] or small angle neutron scattering (SANS),[15] in several compressed traditional organic solvents; however, only a few such measurements have been performed in compressed CO_2.[16] SANS has been the main technique used to investigate CO_2 solubility of fluoropolymers such as hexafluoropropylene oxide (HFPPO)[17] and poly(1,1-dihydroperfluorooctyl acrylate) (PFOA).[16,18−20] PFOA was also studied by SLS in CO_2, and the solvent quality was demonstrated to improve with CO_2 density.[16] The universal dependence of A_2 on the polymer interaction parameter $N^{1/2}(T - T_\theta)/T$ is predicted theoretically,[21] where N is the number of Kuhn segments per chain, T the absolute temperature, and T_θ the theta temperature. This universal behavior of A_2 was verified experimentally in traditional organic solvents[9] and by numerical simulations performed above the theta temperature.[10]

Polysiloxanes were chosen for the present study, because they are easier to characterize in traditional organic solvents, although they are less soluble in CO_2 than most fluoropolymers. Previous polydimethyl siloxane (PDMS) studies performed in CO_2 focused mainly on the boundaries between poor and good solvent regimes. These investigations were performed by either cloud point curves,[22] dynamic light scattering (DLS),[23] or SANS;[24,25] however, they did not give quantitative and direct data related to polymer−solvent interactions as provided by the A_2 measurements.

In this paper, we report the A_2 values for PDMS solutions in both benzene and compressed CO_2. The investigation in benzene was performed to characterize the polymer samples. The studies in CO_2 were performed over a large range of experimental conditions to provide quantitative information related to solvent quality variation as the temperature or density of the CO_2 was changed independently. PDMS samples with three different molecular weights ($M_w = 17$, 24, and 31 kDa) were studied via DLS, whereas only samples with the two larger molecular weights were studied by SLS.

† Part of the special issue "Tomas Baer Festschrift".

* Authors to whom correspondence should be addressed. E-mail addresses: desimone@unc.edu, mr@unc.edu, madam@unc.edu.

‡ University of North Carolina at Chapel Hill.

§ North Carolina State University.

10.1021/jp0481308 CCC: $27.50
Published on Web 10/09/2004

II. Experimental Section

II.1. Sample Characteristics and Procedure. PDMS samples were purchased from Polymer Standards. The polydispersity of all of the samples was 1.05, which was low enough for its influence on the results to be neglected, because we are not concerned with phase separation. Benzene (Fisher) and high-purity CO_2 (Air Products, SFC grade) were used as solvents. All the products were used as received, without further treatment or purification.

The polymer concentration was determined using gravimetric methods. The scattering experiments were first performed at a CO_2 density that was set at room temperature, and then the temperature was varied by heating the cell while keeping the amount of polymer and CO_2 constant. PDMS samples with low molecular weights (M_w = 17, 24, and 31 kDa) were chosen because they are more soluble in CO_2, therefore making it easier to avoid temperatures and pressures where phase separation may occur. The reproducibility of the measurements was checked by reloading the cell with polymer and CO_2 and using an equilibration time that was 30 min longer than the time required to reach stable values of temperature, pressure, and scattered and transmitted intensities. Details of the experimental procedure are given in the Supplemental Information.

II.2. Apparatus and Light Scattering Cells. Static and dynamic light scattering (SLS and DLS, respectively) experiments were performed with equipment from Brookhaven Instruments, including a spectrometer that was equipped with a polarized Ar^+ ion laser operating at a wavelength of $\lambda = 514$ nm, and a working output power that varied from 20 mW to 200 mW.

For high-pressure studies, a light scattering cell was manufactured in brass with sapphire windows, which was designed to operate at pressures up to 68.9 MPa. The cell fits on the top of the Brookhaven goniometer and allows measurements at angles of 45°, 90°, and 135°. The polymer concentration in the cell can be reduced by increasing the inner volume from 8.3 mL to 47.3 mL, using a stainless-steel cylindrical piston. A syringe pump (ISCO, model 260D) was used to deliver CO_2 to the cell. CO_2 was filtered by a Swagelok Tee-Type Filter (0.5 μm). The pressure was monitored with a pressure transducer (Sensotec A-205, precision of 1% full scale). The temperature of the sample was monitored by two Type-K thermocouples that were connected with a temperature control unit (Omega CN77353-A2). Temperature control of the cell was maintained within a precision and stability of 0.5 °C using a circulating fluid temperature bath.

II.3. Light Scattering Principles. The relevant parameter for scattering studies is the scattering wave vector q, which is defined by

$$q = \frac{4\pi n_s}{\lambda} \sin\left(\frac{\theta}{2}\right) \tag{1}$$

where θ is the scattering angle and n_s is the refractive index of the solvent. The n_s value for the CO_2 investigation was calculated for every experimental condition[26] (the values are listed in the Supplemental Information).

II.3.1. Static Light Scattering (SLS). In the SLS experiments and for various polymer concentrations C, the relative excess of scattered intensity ($I(q,C)$) was measured, with respect to the solvent. The scattering data were converted to the excess Rayleigh's ratio, $R(q,C)$. In CO_2, the $R(q,C)$ value has been corrected using a toluene sample reference, $R(q,C) = I(q,C) R_\theta^{\text{toluene}} I_{CO_2}/I_{\text{toluene}}$, for which the Rayleigh ratio is $R_\theta^{\text{toluene}} = 3.21 \times 10^{-5}$ cm^{-1} at 25 °C for $\lambda = 514$ nm. For the experiments performed in benzene, a Rayleigh ratio of $R_\theta^{\text{benzene}} = 3.00 \times 10^{-5}$ cm^{-1} for $\lambda = 514$ nm was used.[27] The dependence of excess Rayleigh ratio $R(q,C)$ on polymer concentration C and scattering wavevector q is given by[28]

$$\frac{KC}{R(q,C)} = \frac{1}{M_w P(q)} + 2A_2 C + ... \tag{2}$$

$$\frac{1}{P(q)} = 1 + \frac{1}{3} R_g{}^2 q^2 + ... \tag{3}$$

where A_2 is the second virial coefficient that describes the polymer−solvent interactions, $P(q)$ the polymer scattering factor, and R_g the radius of gyration. As will be shown later, the size of the polymers studied were such that the maximum value of qR_g was on the order of 0.1. Thus, the scattered intensity was independent of q and the experiments were performed at $\theta \approx 90°$. $I(q,C)$ was determined by averaging 20 measurements over a scattering angle interval of 10°. K is an optical constant, defined as[28]

$$K = \frac{4\pi^2 n_s^2 (\mathrm{d}n/\mathrm{d}C)^2}{\lambda^4 N_A} \tag{4}$$

where $\mathrm{d}n/\mathrm{d}C$ is the refractive index increment and N_A is Avogadro's number. For PDMS in benzene, $\mathrm{d}n/\mathrm{d}C = 0.0919$ mL/g at 25 °C.[29,30] Because the values of $\mathrm{d}n/\mathrm{d}C$ for polymers in CO_2 are not available, $\mathrm{d}n/\mathrm{d}C$ was calculated for every CO_2 density of interest, based on the expansion of the solution refractive index, n_{solution}, as a function of the polymer concentration:

$$n_{\text{solution}} = n_{CO_2} + \frac{\mathrm{d}n}{\mathrm{d}C} C + ... \tag{5}$$

where n_{CO_2} is the refractive index of the CO_2. The refractive index $\mathrm{d}n/\mathrm{d}C$ was approximated by linear interpolation between the two pure components:

$$\frac{\mathrm{d}n}{\mathrm{d}C} \approx \frac{n_{CO_2} - n_{\text{PDMS}}}{\rho_{\text{PDMS}}} \tag{6}$$

where n_{PDMS} is the refractive index of the polymer (1.405) and ρ_{PDMS} is the PDMS density (0.97 g/mL).[31]

II.3.2. Dynamic Light Scattering (DLS). In DLS experiments, the time autocorrelation function of the scattered intensity ($g^{(2)}(t,q)$) was measured and expressed in terms of the field autocorrelation function ($g^{(1)}(q,t)$):[28]

$$g^{(2)}(q,t) = \frac{\langle I^*(q,0) I(q,t) \rangle}{\langle I^*(q,0) \rangle^2} = 1 + A|g^{(1)}(q,t)|^2 \tag{7}$$

where A is an instrument constant. The values of A in our experiments were in the range of 0.25−0.5, depending upon the number of coherence areas selected. The electric field autocorrelation function is defined as

$$g^{(1)}(q,t) = \frac{\langle E^*(0) E(t) \rangle}{\langle E(0)^2 \rangle} \tag{8}$$

where $E(t)$ and $E(0)$ represent the scattered electric field at time t and time $t = 0$, respectively.

For all solutions studied in this work, the exponential autocorrelations were characterized by a single characteristic

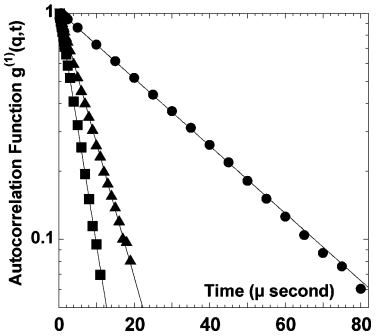

Figure 1. Semilogarithmic plot of the field autocorrelation functions ($g^{(1)}(q,t)$) obtained at 25 °C for PDMS samples with a molecular weight of M_w = 31 kDa, a CO_2 density of 1.04 g/mL, and a polymer concentration of C = 0.0232 g/mL. Different sets of symbols correspond to wavevectors: (■) 0.0284, (▲) 0.0216, and (●) 0.0107 nm^{-1}.

time (τ_c), which is inversely proportional to q^2. In this case, the field autocorrelation function $g^{(1)}(q,t)$ is

$$g^{(1)}(q,t) = \exp\left(-\frac{t}{\tau_c}\right) = \exp(-D_c q^2 t) \qquad (9)$$

D_c is the mutual diffusion coefficient. Experimentally, D_c was determined to be independent of q and was averaged over three scattering angles: 41°, 90°, and 137°. For illustrative purposes, experimental field autocorrelation functions $g^{(1)}(q,t)$ are shown in semilogarithmic representation in Figure 1, where the straight lines correspond to the fitted curves obtained using eq 9.

The mutual diffusion coefficient varies linearly with the polymer concentration.

$$D_c = D_0(1 + k_d C + ...) \qquad (10)$$

where k_d is the diffusional second virial coefficient, which contains both hydrodynamic and thermodynamic interactions,[32] and D_0 is the translational diffusion coefficient of the polymer at infinite dilution, which is related to the hydrodynamic radius, R_h, through the Stokes−Einstein relation:

$$D_0 = \frac{kT}{6\pi\eta_s R_h} \qquad (11)$$

where k is the Boltzmann constant, T is the absolute temperature, and η_s is the solvent viscosity, which is a function of both temperature and solvent density (see Supplemental Information for tables of data).

III. Results

III.1. Static Light Scattering. SLS measurements in benzene and in CO_2 were conducted to determine the second virial coefficient (A_2) and the molecular weights of the PDMS samples under various experimental conditions.[33] Only the data obtained in CO_2 are fully presented herein. CO_2 density and temperature were varied separately, over ranges of 0.97−1.01 g/mL and 25−54 °C, respectively.

The molecular weights of the PDMS samples were deduced from the extrapolation to zero concentration of the KC/R measurements, whereas their concentration dependence allowed for the determination of the value of A_2 (see eq 2).

The expected linear variation of KC/R with C is shown in Figure 2. This behavior was observed for every experimental condition when either temperature or CO_2 density was varied.

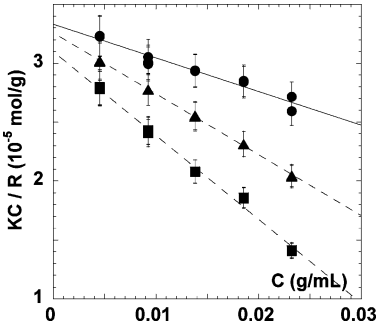

Figure 2. KC/R as a function of the polymer concentration C for PDMS samples with M_w = 31 kDa at a CO_2 density of 0.97 g/mL and three different temperatures: (■) 25, (▲) 37, and (●) 54 °C.

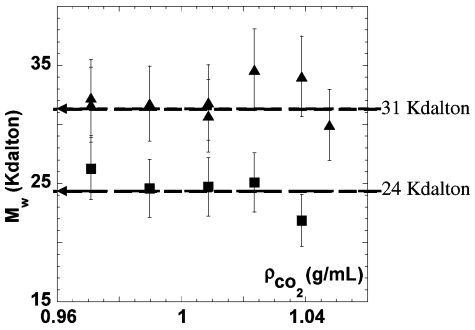

Figure 3. Molecular weights determined by light scattering in CO_2 at 25 °C, plotted as a function of the CO_2 density for two samples: (■) 24 and (▲) 31 kDa. Dashed lines at 24 and 31 kDa correspond to the molecular-weight values measured in benzene.

For the sake of clarity, Figure 2 presents only some of the measurements performed for one of the molecular weights analyzed.

The molecular weights of the PDMS samples were determined in benzene and in CO_2. The molecular weights determined as a function of CO_2 density are shown in Figure 3 (see Supplemental Information for tables of data). There is good agreement (within 10%) between the determination of the molecular weights of the PDMS samples measured in benzene at 25 °C and in CO_2 at every experimental condition (M_w = 24 and 31 kDa). This agreement in the molecular weight between the different solvents supports the calculation of the refractive index increment, dn/dC (see eq 6). In addition, this confirms that phase separation does not occur in the range of temperature and density scanned in this experiment.

From the concentration dependence of KC/R, the product of the second virial coefficient and the molecular weight (M_wA_2) can be determined. M_wA_2 was observed to vary significantly with temperature as the CO_2 density was kept constant (see Figure 4A and B).

For each molecular weight and each CO_2 density, the value of M_wA_2 increases with temperature. In Figure 4B, the filled symbols correspond to data measured with an equilibration time 30 min longer than that for the data represented by empty symbols. The results were observed to be reproducible within the error bars.

When the CO_2 density was increased from 0.97 g/mL to 1.01 g/mL, the M_wA_2 values increased and the temperature influence became stronger (see Figure 4A and B). This trend was observed for both of the different-molecular-weight PDMS samples that were analyzed. Although the M_wA_2 values remained negative, in the range of experimental conditions investigated, the linear extrapolation of the variation of M_wA_2 with temperature was

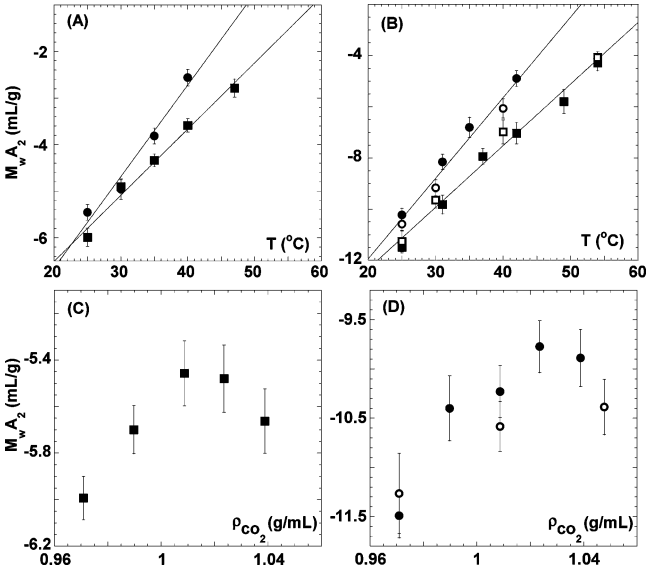

Figure 4. (A and B) Variation of the second virial coefficient multiplied by the molecular weight, M_wA_2, as a function of the temperature for CO_2 densities of 0.97 g/mL (square symbols) and 1.01 g/mL (circular symbols); panel A shows data for a PDMS sample with a molecular weight of 24 kDa, whereas panel B shows data for a PDMS sample with a molecular weight of 31 kDa. (C and D) M_wA_2 as a function of the CO_2 density at 25 °C; panel C shows data for a PDMS sample with a molecular weight of 24 kDa, whereas panel D shows data for a PDMS sample with a molecular weight of 31 Kdalton. Empty and filled symbols correspond to the first and second runs, respectively.

TABLE 1: Theta Temperatures as a Function of the CO_2 Density (ρ_{CO_2}) for the Two PDMS Molecular Weights (M_w)

	theta temperature, $T_{\theta extrap}$ (°C)	
ρ_{CO_2} (g/mL)	$M_w = 24$ kDa	$M_w = 31$ kDa
0.97	66 ± 4	71 ± 2
1.01	54 ± 6	58 ± 4

used to determine the theta temperature, T_θ, i.e., the temperature at which $A_2 = 0$ (see Table 1).

The precision of such an extrapolation is limited by the temperature interval between T_θ and the higher temperature at which experiments can safely be performed. T_θ is a function of CO_2 density: it changes by ~12 °C as the CO_2 density varies within a range of 0.97−1.01 g/mL. The uncertainty in the estimate of T_θ does not allow us to establish if it is dependent on the PDMS molecular weight.

At constant temperature, the variation of M_wA_2 with CO_2 density was investigated (see Figure 4C and D). The CO_2 density effect can be considered to be nonmonotonic; as the solvent density was increased, M_wA_2 first increased and then decreased for density higher than 1.01 g/mL. To confirm this decrease of solvent quality, an investigation over a larger range of density would be required. We could not perform experiments in this higher pressure range, because of both the pressure limit of the ISCO pump and the safety limit imposed by the present scattering setup. The nonmonotonic behavior of M_wA_2 was observed for the two different-molecular-weight PDMS samples and indicates that there is no CO_2 theta density (ρ_θ) at 25 °C.

III.2. Dynamic Light Scattering. The DLS technique can be used to measure the mutual diffusion of the polymer, D_c. Its extrapolation to zero concentration, D_0, is related to the hydrodynamic size of the polymers, whereas the concentration dependence of D_c is related to the interactions (see eqs 10 and 11).

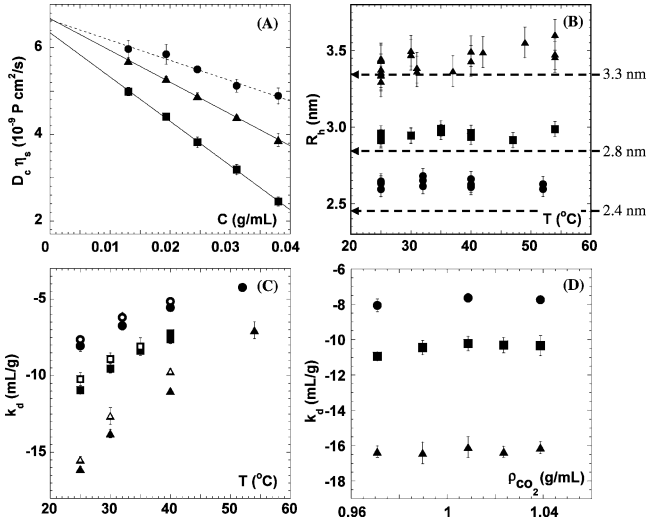

Figure 5. (A) Diffusion coefficients multiplied by the CO_2 viscosity plotted as a function of the polymer concentration, measured at various temperatures ((■) 25, (▲) 40, and (●) 54 °C) for a PDMS sample with a molecular weight of 31 kDa. (B) Hydrodynamic radii as a function of temperature (dashed lines indicate R_h values measured in benzene) (PDMS molecular weight of (●) 17, (■) 24, and (▲) 31 kDa). (C) Variation of k_d, with temperature; data for CO_2 densities of 0.97 and 1.01 g/mL are denoted by filled symbols and empty symbols, respectively (PDMS molecular weight of (●) 17, (■) 24, and (▲) 31 kDa). (D) Variation of k_d with the CO_2 density at 25 °C (PDMS molecular weight of (●) 17, (■) 24, and (▲) 31 kDa).

TABLE 2: Hydrodynamic Radius (R_h) in CO_2, Averaged over Various Temperatures and Solvent Densities

	average R_h (±0.2 nm)	
M_w (kDa)	in CO_2	in benzene[a]
17	2.6	2.4
24	2.9	2.8
31	3.5	3.3

[a] R_h value in benzene was measured at 25 °C.

Figure 5A illustrates the variation of $D_c\eta_s$ with polymer concentration C. Multiplying the diffusion coefficient D_c by η_s accounts for the variation of the solvent viscosity with temperature and density (see eq 11). In all cases, D_c was determined to vary linearly with C. Figure 5B presents the hydrodynamic radius, R_h, obtained from the extrapolation of D_c to zero concentration using eq 11. Data were obtained at different CO_2 densities and different temperatures. Three molecular weights[33] were studied by DLS; the hydrodynamic radii were determined to be independent of both temperature and solvent density. The sizes of these polymers were also measured in benzene. The hydrodynamic sizes in CO_2 are systematically larger than those in benzene; however, the difference between the two data sets are comparable to the experimental precision (±0.2 nm) (see Table 2 and dashed lines in Figure 5B).

The diffusional "second virial" coefficient (k_d) was extracted from Figure 5A (see eq 10), and the results were plotted as a function of temperature in Figure 5C (see also Supplemental Information). For all three PDMS samples, k_d increases as the temperature increases at constant CO_2 density. A similar temperature effect was observed at other CO_2 densities. The coefficient k_d contains both hydrodynamic and thermodynamic contributions,[32] and the solvent quality improvement with temperature measured by DLS was qualitatively consistent with the changes in the thermodynamic interactions, M_wA_2, as measured by SLS (compare Figures 5C, 4A, and 4B). The

temperature variation of M_wA_2 was determined to be stronger at higher CO_2 densities, whereas the temperature variation of k_d was determined not to be very sensitive to CO_2 density. When the CO_2 density was increased from 0.94 g/mL to 1.01 g/mL, the variation of k_d with temperature did not change significantly (compare empty and filled symbols in Figure 5C). The variation of k_d with the solvent density at 25 °C is plotted in Figure 5D. Over the studied range of parameters, k_d was determined to be independent of solvent density within the experimental uncertainty.

IV. Discussion

IV.1. Theta Temperature and Interactions. The light scattering data presented previously can be compared to the phase behavior of PDMS in supercritical CO_2 ($scCO_2$), which was previously investigated by Melnichenko and co-workers[24] using SANS for similar and higher molecular weights. They probed the transition from the θ conditions to the good solvent regime, as a function of both temperature and solvent density. Their study was performed at the overlap concentration, and both the radius of gyration and the correlation length were measured. Interestingly, note that, despite a range of experimental conditions (ranging from the good solvent regime to the conditions where the polymer precipitated), Melnichenko et al. did not observe a size reduction of the polymer coils. They found that the transition temperature decreased as the CO_2 density increased (70 °C at 0.93 ± 1 g/mL, and 65 °C at 0.95 g/mL), which supports the results presented herein (see Table 1).

The variation of T_θ with solvent density or pressure is not a specific property of either PDMS or $scCO_2$. Indeed, Dickson et al. studied the phase diagram of PFOMA samples of various molecular weights and reported a decrease of T_θ with increasing CO_2 density, which is consistent with improvement of the solvent quality.[34] A variation of the θ conditions with either the pressure or the solvent density has also been reported in traditional organic solvents for several polymer systems, such as polystyrene (PS) in trans-decalin[14] and cyclohexane,[13] polyisobutylene in 2-methylbutane,[13] and PDMS in cyclohexyl bromide.[12]

By investigating the variation of the correlation length as a function of CO_2 pressure at constant temperature,[24] it was experimentally observed that a narrow single phase solvent density region can be surrounded by two phase boundaries, reachable by either decreasing or increasing the solvent density. This decrease of PDMS miscibility at both high and low CO_2 density, measured by SANS,[24] is consistent with the trend observed in Figure 4C and D, where the second virial coefficient A_2 first increases as CO_2 density increases and then starts to decrease for CO_2 densities higher than 1.01 g/mL.

The solvent quality information provided in the present work by SLS and DLS can be compared. As opposed to A_2 behavior, no maximum value of k_d, as a function of CO_2 density, is observed. However, when temperature is increased, the variation of A_2 and k_d indicates an improvement of the polymer solubility in compressed CO_2 (see Figures 4A, 4B, and 5C).

IV.2. Second Virial Coefficients. *IV.2.1. Positive Second Virial Coefficient.* Thermodynamic and conformational properties of polymer solutions have been studied for a long time.[35,36] In 1966,[9] Berry experimentally confirmed, using PS samples, that the positive second virial coefficient is simply related to three parameters: the unperturbed state in which the conformation of a chain molecule is described by random walk statistics, the number of effective segments, and the mutually excluded volume for any pair of segments. The second virial coefficient, A_2, is a universal function[21] of the interaction parameter, z:

$$\frac{A_2 M_w^{1/2} M_0^{3/2}}{N_A b^3} = C_1 f(z) \tag{12}$$

where N_A is Avogadro's number, $M_0 = 381$ Da and $b = 13$ Å are the mass and length of the Kuhn segment, respectively.[21] The interaction parameter is defined as[21]

$$z = C_2 N^{1/2} \tau = C_2 N^{1/2} \left(1 - \frac{T_\theta}{T}\right) \tag{13}$$

where T is the solution temperature, τ is its relative deviation from T_θ, N is the number of Kuhn segments in the polymer chain, and both C_1 and C_2 are proportionality coefficients. The limiting behaviors of the universal function is $f(z) = z$ for $z \ll 1$ (corresponding to the θ solvent) and $f(z) = z^{0.588}$ for $z \gg 1$ (good solvent limit). This form of universal relation assumes that (i) the interaction parameter is a simple function of T and T_θ, as described by eq 13; (ii) the Kuhn length b is independent of solvent; and (iii) the chain is long enough for end-group effects to be neglected.

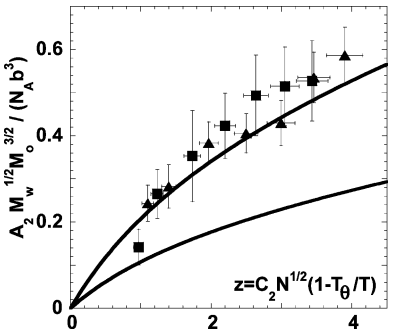

Figure 6. Normalized second virial coefficient plotted as a function of the interaction parameter for PDMS samples with molecular weights of (■) 24 and (▲) 31 kDa in benzene. The data previously obtained in traditional organic solvents (not shown) are located between the two solid curves.[9,37−39]

Experimentally, this behavior was verified for PS in both Decalin and toluene.[9] More recently,[10] a Monte Carlo simulation was used to investigate the properties of polymer chains. The coefficients C_1 and C_2 were determined to be independent of the system under consideration and equal to 0.20 ± 0.02 and 2.02 ± 0.08, respectively. Various chain lengths and segment−segment interactions were used and simulation data were collapsed onto the experimental data without the use of additional adjustable parameters. As a consequence, this universal model is expected to apply to all uncharged linear polymers in θ and good solvents.

The aforementioned approach was used to treat the PDMS data collected in benzene where A_2 remains positive. The theta temperature of $T_\theta = -7$ °C and the length of a Kuhn segment, $b = 14$ Å, were previously reported in the literature.[29]

Figure 6 presents a good agreement of our data on PDMS in benzene with the universal dependence of the second virial coefficient (eq 12) confirmed in earlier experiments on polymers in organic solvents.[10,37] In benzene, the amplitude of the interaction parameter, z, is >1, indicating that most of the measurements were performed in the good solvent regime.

IV.2.2. Negative Second Virial Coefficient. There are only few experimental studies of the parameter A_2 for polymers in solutions below their theta temperature. Theoretical models predict a universal curve when $A_2 M_w^{1/2} M_0^{3/2}/(N_A b^3)$ is plotted as

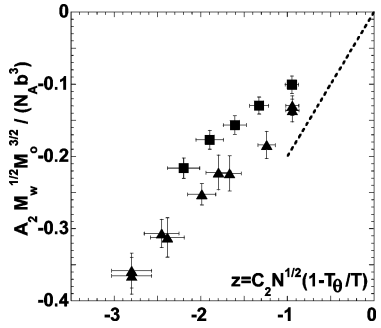

Figure 7. Reduced second virial coefficient of PDMS samples with molecular weights of (■) 24 and (▲) 31 kDa in CO_2 at a density of 0.97 g/mL. Linear extrapolation of the universal curve into the negative A_2 regime is represented by the dashed line.

a function of the interaction parameter.[9,40,41] The most studied system in the negative A_2 region is PS in cyclohexane.[42] However, none of the theoretical models successfully describe the variation of A_2 for PS in cyclohexane below its theta temperature. Instead, the experimental data for different molecular weights do not collapse onto the same "universal curve".

The experimental results obtained with PDMS in CO_2 solutions at a solvent density of 0.97 g/mL are presented in Figure 7. The dashed line is the linear extrapolation of the universal curve, $C_1 f(z) = C_1 z$, into the negative A_2 regime. As z becomes more negative, the experimental variation of A_2 with z is weaker than predicted by this extrapolation. Note that linear extrapolation is not expected to be valid for $z < -1$. The data for PDMS in CO_2 did not collapse onto one single curve. An increase in molecular weight results in a decrease in A_2 values at a constant interaction parameter z. This behavior is opposite to that reported for the PS−cyclohexane system.[42] Further study is needed for a deeper understanding of this nonuniversal behavior. Two possible sources of nonuniversality can be identified:

(1) The absence of collapse of the normalized A_2 values[43,44] and the molecular weight variation of the T_θ value observed for PDMS in CO_2 (see Table 1) may be explained by the contribution of the end group[45−50] to the effective polymer−solvent interactions. Although not yet carefully investigated under sub-θ conditions, the end group effect has been proposed to explain the molecular-weight variation of T_θ observed with various short polymer chains in several solvents, the strong molecular weight dependence of A_2 in the PαMS−cyclohexane system,[43,46] and the very weak molecular weight dependence of A_2 for PS−cyclohexane.[47,51]

(2) The approximation of the interaction parameter by a simple function such as eq 13 is not necessarily correct and must be carefully re-evaluated for systems with large absolute values of the interaction parameter z. This approximation has been verified above T_θ for some generic polymeric systems; however, it is expected to be valid only very close to T_θ. Withers et al.[52] noticed that an additional adjustable parameter may be required to collapse experimentally measured and numerically simulated swelling coefficients.[53,54]

IV.3. Polymer Size. Good agreement between the PDMS chain sizes determined in benzene and CO_2 has been achieved (see Table 2). This is consistent with the fact that below T_θ, neither phase separation nor polymer aggregation was observed within the range of experimentally studied conditions for PDMS in CO_2. The hydrodynamic radii also agree well with data obtained for similar molecular weights in bromocyclohexane at T_θ, which were 2.9 and 3.6 nm for the PDMS samples with $M_w = 21.2$ and 31.9 kDa, respectively.[55] In a θ solvent, the end-to-end distance, R_0, is proportional to the square root of the molecular weight:

$$R_0 = \sqrt{6}\alpha_{gh} R_h \tag{14}$$

where α_{gh} is the ratio of the radius of gyration to the hydrodynamic radius ($\alpha_{gh} = 1.27$ at T_θ).[56] For PDMS in various θ solvents, $10^2 R_0/\sqrt{M_w}$ is equal to 6.1 ± 0.1 nm mol$^{1/2}$ g$^{-1/2}$.[29,30] From Table 2, we obtain the ratio $10^2 R_0/\sqrt{M_w}$ for PDMS. Its value was equal to 6.1 ± 0.5 nm mol$^{1/2}$ g$^{-1/2}$ in CO_2 and 5.6 ± 0.5 nm mol$^{1/2}$ g$^{-1/2}$ in benzene.

We conclude that, within the error bars, the sizes of PDMS chains are not affected by the solvent temperature or the CO_2 density over the entire range of experimental conditions investigated in this work. This may be explained by the fact that the expected hydrodynamic swelling was too small, in comparison to the experimental precision. A similar conclusion is reached for the swelling of our PDMS chains in benzene. To summarize, the absence of a measurable size variation with the experimental conditions is consistent with the fact that the polymers investigated in this study are too small for the change of their size to be larger than the experimental precision.

V. Conclusion

In this paper, we report the results of static light scattering (SLS) and dynamic light scattering (DLS) experiments in both compressed and supercritical CO_2. The results show that both the size and the average molecular weight measured in CO_2 and benzene are in good agreement. In compressed CO_2, this study was performed below the θ point. The compressed CO_2 solvent quality can be tuned with temperature, as observed by both SLS and DLS. The hydrodynamic radius measured in CO_2 remained equal to the θ size over the entire range of solvent quality that was investigated and was in good agreement with reported data in other θ solvents.

This study provides quantitative information on CO_2 solvent quality over a large range of experimental conditions. The extrapolated theta temperature (T_θ) was determined to be a strong function of CO_2 density and a weaker function of polydimethyl siloxane (PDMS) molecular weight. In the PDMS−CO_2 solution, the strength of the interactions was weaker than predicted and no universal behavior was observed. An end-group contribution to the interactions and the approximation of the expression of the interaction parameter are proposed as contributing to the failure of the universality approach.

In addition, the observed behavior of PDMS in CO_2 was compared with a previous small-angle neutron scattering (SANS) investigation of PDMS. This work confirmed that the CO_2 density is not the only parameter to control polymer solubility and that temperature can have an important role in tuning solubility. Furthermore, an increase in CO_2 density was shown to improve and then reduce the CO_2 solvent quality.

Acknowledgment. The authors would like to thank F. Pinero who engineered the final design of the high-pressure cells. We are also indebted to J. L. Dickson and K. P. Johnston for access to the preprint of their paper. The authors would like to thank the Kenan Center for the Utilization of Carbon Dioxide in Manufacturing for financial support and the NSF Science and Technology Center for Environmentally Responsible Solvent and Processes (under No. CHE-9876674).

Supporting Information Available: Technical details, experimental procedure, and tables of data (PDF). This material is available free of charge via the Internet at http://pubs.acs.org.

References and Notes

(1) Quinn, E. L.; Jones, C. L. *Carbon Dioxide*; Reinhold Publishing Corporation: New York, 1936.

(2) DeSimone, J. M. *Science* **2002**, *297*, 799−803.

(3) Weibel, G. L.; Ober, C. K. *Microelectron. Eng.* **2003**, *65* (1−2), 145−152.

(4) Beckman, E. J. *J. Supercrit. Fluids* **2004**, *28* (2−3), 121−191.

(5) Kirby, C. F.; McHugh, M. A. *Chem. Rev.* **1999**, *99* (2), 565−602.

(6) Desimone, J. M.; Maury, E. E.; Menceloglu, Y. Z.; Mcclain, J. B.; Romack, T. J.; Combes, J. R. *Science* **1994**, *265* (5170), 356−359.

(7) Sarbu, T.; Styranec, T.; Beckman, E. J. *Nature (London)* **2000**, *405*, 165−168.

(8) O'Neill, M. L.; Cao, Q.; Fang, R.; Johnston, K. P.; Wilkinson, S. P.; Smith, C. D.; Kerschner, J. L.; Jureller, S. H. *Ind. Eng. Chem. Res.* **1998**, *37* (8), 3067−3079.

(9) Berry, G. C. *J. Chem. Phys.* **1966**, *44* (12), 4550−4564.

(10) Withers, I. M.; Dobrynin, A. V.; Berkowitz, M. L.; Rubinstein, M. *J. Chem. Phys.* **2003**, *118* (10), 4721−4732.

(11) McDonald, C. J.; Claesson, S. *Chem. Scr.* **1976**, *9* (1), 36−46.

(12) Kubota, K.; Kubo, K.; Ogino, K. *Bull. Chem. Soc. Jpn.* **1976**, *49* (9), 2410−2418.

(13) Gaeckle, D.; Patterson, D. *Macromolecules* **1972**, *5* (2), 136−141.

(14) Schulz, G. V.; Lechner, A. Influence of Pressure and Temperature (Chapter 12). In *Light Scattering from Polymer Solutions*; Huglin, M. B., Ed.; Academic Press: New York, 1972.

(15) DiNoia, T. P.; Kirby, C. F.; van Zanten, J. H.; McHugh, M. A. *Macromolecules* **2000**, *33* (17), 6321−6329.

(16) Buhler, E.; Dobrynin, A. V.; DeSimone, J. M.; Rubinstein, M. *Macromolecules* **1998**, *31* (21), 7347−7355.

(17) Londono, J. D.; Dharmapurikar, R.; Cochran, H. D.; Wignall, G. D.; McClain, J. B.; Betts, D. E.; Canelas, D. A.; DeSimone, J. M.; Samulski, E. T.; Chillura-Martino, D.; Triolo, R. *J. Appl. Crystallogr.* **1997**, *30* (2), 690−695.

(18) McClain, J. B.; Betts, D. E.; Canelas, D. A.; Samulski, E. T.; DeSimone, J. M.; Londono, J. D.; Cochran, H. D.; Wignall, G. D.; ChilluraMartino, D.; Triolo, R. *Science* **1996**, *274* (5295), 2049−2052.

(19) McClain, J. B.; Londono, D.; Combes, J. R.; Romack, T. J.; Canelas, D. A.; Betts, D. E.; Wignall, G. D.; Samulski, E. T.; DeSimone, J. M. *J. Am. Chem. Soc.* **1996**, *118* (4), 917−918.

(20) Chillura-Martino, D.; Triolo, R.; McClain, J. B.; Combes, J. R.; Betts, D. E.; Canelas, D. A.; DeSimone, J. M.; Samulski, E. T.; Cochran, H. D.; Londono, J. D.; Wignall, G. D. *J. Mol. Struct. (THEOCHEM)* **1996**, *383* (1−3), 3−10.

(21) Rubinstein, M.; Colby, R. H. *Polymer Physics*; Oxford University Press: New York, 2003.

(22) Xiong, Y.; Kiran, E. *Polymer* **1995**, *36* (25), 4817−4826.

(23) Liu, K.; Kiran, E. *J. Supercrit. Fluids* **1999**, *16* (1), 59−79.

(24) Melnichenko, Y. B.; Kiran, E.; Wignall, G. D.; Heath, K. D.; Salaniwal, S.; Cochran, H. D.; Stamm, M. *Macromolecules* **1999**, *32* (16), 5344−5347.

(25) Melnichenko, Y. B.; Brown, W.; Rangelov, S.; Wignall, G. D.; Stamm, M. *Phys. Lett. A* **2000**, *268* (3), 186−194.

(26) Burns, R. C.; Graham, C.; Weller, A. R. M. *Mol. Phys.* **1986**, *59* (1), 41−64.

(27) The values of the Rayleigh ratio for toluene and benzene at a wavelength of $\lambda = 514$ nm are obtained by interpolation of the data from the following references: Coumou, J. *J. Colloid Sci.* **1960**, *15*, 408−417; Coumou, D. J.; Mackor, E. L.; Hijmans, J. *Trans. Faraday Soc.* **1964**, *60*, 1539−1547.

(28) Chu, B. *Laser Light Scattering: Basic Principles and Practice*; Academic Press: Boston, 1991.

(29) Brandrup, J.; Immergut, E. H. *Polymer Handbook*; Wiley: New York, 1989.

(30) Nilsson, R.; Sundelof, L.-O. *Makromol. Chem.* **1963**, *66*, 11−18.

(31) Huglin, M. B. *J. Appl. Polym. Sci.* **1965**, *9*, 3963−4001, 4003−4024.

(32) Yamakawa, H. *Modern Theory of Polymer Solutions*; Harper and Row: New York, 1970.

(33) Three PDMS molecular weights were investigated. For the lowest-molecular-weight samples studied in CO_2, the beam was partially obturated by the pinhole in front of the scattering cell. This technical error prevent the calculation of the scattered intensity ($I(q,C)$), but it did not alter the DLS measurements that are presented.

(34) Dickson, J. L.; Ortiz-Estrada, C.; Alvarado, J. F. J.; Hwang, H. S.; Sanchez, I. C.; Luna-Barcenas, G.; Lim, K. T.; Johnston, K. P. *J. Colloid Interface Sci.* **2004**, *272*, 444−456.

(35) Cotton, J. P.; Nierlich, M.; Boue, F.; Farnoux, B.; Daoud, M.; Jannink, G.; Duplessix, R.; Picot, C. *J. Chem. Phys.* **1976**, *65*, 1101−1108.

(36) de Gennes, P.-G. *Scaling Concepts in Polymer Physics*; Cornell University Press: Ithaca, NY, 1979.

(37) Berry, G. C.; Casassa, E. F.; Liu, P. Y. *J. Polym. Sci. B* **1987**, *25*, 673−696.

(38) Nakamura, Y.; Norisuye, T.; Teramoto, A. *Macromolecules* **1991**, *24* (17), 4904−4908.

(39) Nakata, M. *Phys. Rev. E* **1995**, *51* (6), 5770−5775.

(40) Grosberg, A. Y.; Kuznetsov, D. V. *Macromolecules* **1992**, *25* (7), 1970−1979, 1980−1990, 1991−1995, 1996−2003.

(41) Rabin, Y. *J. Chem. Phys.* **1983**, *79* (8), 3988−3990.

(42) Perzynski, R.; Delsanti, M.; Adam, M. *J. Phys. (Paris)* **1987**, *48* (1), 115−124.

(43) Li, J.; Harville, S.; Mays, J. W. *Macromolecules* **1997**, *30* (3), 466−469.

(44) A collapse of the data using a different universal plot below the theta point was reported by Li et al. Similar approaches do not collapse the PDMS in CO_2 data and PS in cyclohexane data.

(45) Yamakawa, H. *Macromolecules* **1992**, *25* (7), 1912−1916.

(46) Tokuhara, W.; Osa, M.; Yoshizaki, T.; Yamakawa, H. *Macromolecules* **2003**, *36* (14), 5311−5320.

(47) Einaga, Y.; Abe, F.; Yamakawa, H. *Macromolecules* **1993**, *26* (23), 6243−6250.

(48) Abe, F.; Einaga, Y.; Yamakawa, H. *Macromolecules* **1994**, *27* (12), 3262−3271.

(49) Yamakawa, H.; Yoshizaki, T. *J. Chem. Phys.* **2003**, *119* (2), 1257−1270.

(50) Yamakawa, H.; Yoshizaki, T. *J. Chem. Phys.* **2003**, *118* (6), 2911−2918.

(51) Perzynski, R. Ph.D. Thesis, Universite Paris VI, Paris, France, 1984.

(52) Withers, I. M.; Dobrynin, A. V.; Rubinstein, M., manuscript in preparation.

(53) Hayward, R. C.; Graessley, W. W. *Macromolecules* **1999**, *32* (10), 3502−3509.

(54) Hayward, R. C.; Graessley, W. W. *Macromolecules* **1999**, *32* (10), 3510−3517.

(55) Horita, K.; Sawatari, N.; Yoshizaki, T.; Einaga, Y.; Yamakawa, H. *Macromolecules* **1995**, *28* (13), 4455−4463.

(56) Schmidt, M.; Burchard, W. *Macromolecules* **1981**, *14* (1), 210−211.

(57) Perzynski, R.; Adam, M.; Delsanti, M. *J. Phys. (Paris)* **1982**, *43* (1), 129−135.